Role of molecular mixing on the stiffness of polymer:fullerene bulk heterojunction films

Adam D. Printz, Suchol Savagatrup, Daniel Rodriquez, Darren J. Lipomi *

Department of NanoEngineering, University of California, San Diego, 9500 Gilman Drive, Mail Code 0448, La Jolla, CA 92093-0448, United States

ABSTRACT

Bulk heterojunction films, which typically comprise a polymer donor and fullerene acceptor, are considerably stiffer than films of the neat polymer. The increase in stiffness upon blending is dependent on the miscibility of the polymer and the fullerene, and potentially on the details of molecular mixing, in particular, intercalation of the fullerene molecules between the polymer side chains. This paper describes the effects of molecular mixing on the tensile modulus of polythiophenes in 1:1 blends with [6,6]-phenyl C_{61} butyric acid methyl ester ($PC_{61}BM$). A series of four polymers and their blends with $PC_{61}BM$ are tested using mechanical, spectroscopic, and photovoltaic device-based measurements to determine if it is possible to predict trends in the tensile modulus based on the extent of molecular mixing. The four polymers are poly-2,2′:5′,2″-(3,3″-dihexyl-terthiophene) (PT2T), which forms an amorphous, molecularly mixed composite, poly(2,5-bis(3-tetradecylthiophen-2-yl)thieno[3,2-b]thiophene) (PBTTT), which forms a well ordered blend with bimolecular crystallization, and regioregular poly(3-hexylthiophene) (P3HT) and poly(3-heptylthiophene) (P3HpT), which form a ternary blend with an amorphous mixed phase. The tensile moduli are measured by the buckling technique and correlations are found between the modulus of the neat polymer and the blends. Although spectroscopic and photovoltaic device-based measurements of $P3HT:PC_{61}BM$ and $PT2T:PC_{61}BM$, along with literature precedent, suggest completely different extents of molecular mixing, they were found to have similar moduli (2.75 ± 0.59 GPa and 2.61 ± 0.39 GPa, after annealing). A strong correlation between the moduli of the blended films and the moduli of the neat polymers suggest that the stiffness of the blend is determined to a large extent by that of the polymer, and is unexpectedly insensitive to the details of molecular mixing, at least for the materials investigated.

© 2014 Elsevier B.V. All rights reserved.

1. Introduction

The pursuit of low-cost, flexible and stretchable organic electronics requires an understanding of the ways in which state-of-the-art electronic properties can coexist with mechanical resilience. Bulk heterojunction (BHJ) photovoltaic devices, which have a photoactive layer comprising donor and acceptor phases mixed on the molecular scale or nanoscale, are the most commonly studied organic photovoltaic (OPV) devices because of their high efficiency and easy processability [1–4]. The extent of molecular mixing (or the size of the phases) in BHJs influences the molecular packing and interfacial interactions, which in turn, greatly affects exciton dissociation, recombination, and charge transport [5,6]. While the relationship between molecular mixing and electronic properties has been studied extensively, the effect of the extent of mixing on the mechanical properties and stability against fracture is not well

known. Improving the mechanical resilience of active materials and interfaces will improve the yield of working devices in roll-to-roll manufacturing, and the lifetime in outdoor, portable, and wearable applications [7–9].

The goal of our experiments was to understand the influence of molecular mixing on the stiffness – i.e., tensile modulus – of BHJ films. In particular, we measured the tensile moduli of four different blends of polymers with main-chains comprising thiophene rings and the methanofullerene [6,6]-phenyl C_{61} butyric acid methyl ester ($PC_{61}BM$), (Fig. 1) whose behaviors in a blend are known in the literature to span a range from an amorphous, molecularly mixed composite ($PT2T:PC_{61}BM$) [10,11], a well ordered blend with bimolecular crystallization ($PBTTT:PC_{61}BM$) [12,13], and two ternary blends with pure or enriched phases separated by mixed phases ($P3HT:PC_{61}BM$ [14,15] and $P3HpT:PC_{61}BM$ [16,17]). The ternary blends are differentiated primarily by the relationship of the glass transition temperature (T_g) of the pure polymer to ambient temperature: T_g for P3HT is close to room temperature [18,19] and is generally reported as stiff (tensile modulus ~ 1 GPa) [20,21], while T_g is below room temperature for

* Corresponding author.
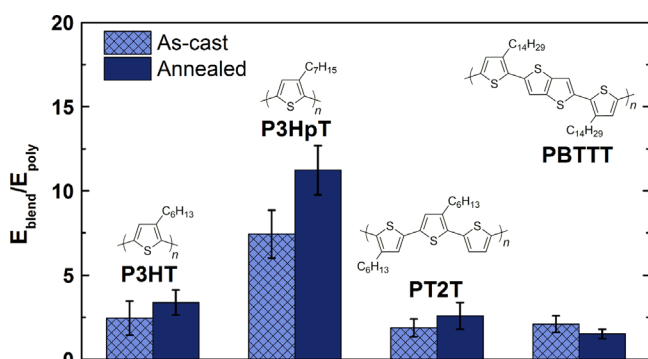E-mail address: dlipomi@ucsd.edu (D.J. Lipomi).

Fig. 1. The ratios of the tensile moduli of as-cast/annealed 1:1 polymer:fullerene blends to as-cast/annealed neat polymers and the chemical structures of the conjugated polymers examined in this work: regioregular poly(3-hexylthiophene) (P3HT), regioregular poly(3-heptylthiophene) (P3HpT), poly-2,2′:5′,2″-(3,3″-dihexyl-terthiophene) (PT2T), and poly(2,5-bis(3-tetradecylthiophen-2-yl)thieno[3,2–b]thiophene) (PBTTT).

P3HpT [16] and is highly elastic (tensile modulus ≤ 0.1 GPa) [16]. While all polymer:fullerene blends reported so far have greater elastic moduli than do the neat polymers [9,11,16,20–22], the factor by which the blend is stiffer than the neat polymer varies over a wide range (Fig. 1). Our goal was to understand the role of molecular mixing by combining our mechanical measurements with knowledge of the well studied microstructures of these four systems. Understanding the effects of molecular mixing on the compliance of BHJs will provide the insight necessary for the selection of materials with mechanical properties appropriate to the application and to mitigate mechanical forms of degradation.

2. Background

The first organic solar cells (OSCs) had a planar heterojunction between a layer of pure donor and a layer of pure acceptor in direct contact [23,24]. This architecture exhibited relatively low efficiencies because of the limited interfacial area between the donor and the acceptor [25]. The discovery of the bulk hetero-junction (BHJ) – an intimately mixed blend of donor and acceptor, which are frequently a conjugated polymer and a soluble fullerene derivative – led to devices exhibiting much higher efficiencies [1–4,26,27]. The advent of BHJs generated significant interest in understanding the extent of molecular mixing to elucidate the relationship between microstructure and electronic performance [5,14,28]. Of equal interest, in terms of the yield of functional devices and their stability in outdoor and portable environments, are the ways in which the morphology of the bulk heterojunc-tion influence the mechanical properties of the composite film [7–9,29,30]. The mechanical aspects of the stability of organic electronic devices have, until recently, received relatively little attention.

The most extensively studied bulk heterojunction blend is P3HT:PC$_{61}$BM [9,14,20–22,31–37]. The current model for this system comprises a ternary blend of a pure polymer phase, a pure (or enriched) fullerene phase, and an amorphous mixed phase of polymer and fullerene [38]. These ternary blends form because PC$_{61}$BM exhibits high solubility in amorphous P3HT, and is excluded from the pure polymer phase, which is well ordered [33,39]. For efficient charge transport, pure phases of both polymer and fullerene are required so that, once separated, charges can travel to the electrodes [14]. Without these percolated networks, losses due to recombination reduce the efficiency. In P3HT:PC$_{61}$BM, the segregated polymer and fullerene phases are believed to account for most of the charge transport in BHJ devices; the

presence of the mixed phase is regarded as deleterious to the efficiency due to the disruption of contiguous pathways for charge transport to the electrodes [14]. Like P3HT, P3HpT – a polythio-phene with a side-chain longer than P3HT by one methylene unit ($n=7$) – is also believed to form ternary blends with PC$_{61}$BM [17]. P3HpT is of particular interest because it has previously been shown to simultaneously display excellent compliance and good photovoltaic characteristics [16].

Very little is known about what, if any, specific molecular interactions are responsible for the solubility of PCBM in amor-phous P3HT. On the other hand, some conjugated polymers, which exhibit lower densities of side chains than do P3HT, contain notches along the polymer chain into which fullerenes can sit [10,13]. This outcome – intercalation – either prevents crystal-lization or produces bimolecular crystallites; the morphology depends on the dimensions of the fullerene compared to the dimensions of the free volume between side chains. For example, the poly(terthiophene) PT2T is similar to P3HT except that every third thiophene in PT2T is without a side chain (and also that the coupling between 3-alkylthiophene rings is tail-to-tail in PT2T and head-to-tail in P3HT, Fig. 1). In neat form, the side chains of PT2T interdigitate, and a highly ordered film is obtained [10]. In bulk heterojunction films, due to the notch between side chains, PT2T is hypothesized to allow intercalation of fullerene along the main chain [10]; intercalation forces the formation of a largely amor-phous molecularly mixed phase. Intercalation of the PC$_{61}$BM likely inhibits cofacial π-stacking as well as lamellar stacking, and this disruption in order produces lowered efficiencies of devices [10,11]. This hypothesis is supported by the much lower power conversion efficiency (PCE) demonstrated in PT2T:PC$_{61}$BM devices when compared to those of P3HT:PC$_{61}$BM, even though the relative positions of the frontier molecular orbitals of PT2T to PC$_{61}$BM suggest that this system might be more efficient than P3HT:PC$_{61}$BM [10].

Miller et al. studied the intercalation of fullerenes between the alkyl solubilizing groups of PBTTT and found that the fullerene solubilizing groups were critical in determining if [13,40]. Mono-functionalized fullerenes, such as PC$_{61}$BM and PC$_{71}$BM, readily intercalated between the side chains of PBTTT, while some multi-functionalized fullerenes, such as bis-PC$_{61}$BM and bis-PC$_{71}$BM, did not intercalate between the side chains due to steric hindrance [13]. The absence of intercalation of multifunctionalized fullerenes was not a generalizable rule, though. Because of its less bulky solubilizing groups, indene-C$_{60}$ bisadduct (ICBA) was found to intercalate [40]. (It should be noted that photovoltaic devices made with ICBA underperformed those made with PC$_{61}$BM because the ICBA preferentially aligned with its side groups parallel to the polymer backbone, which prevented efficient charge transport between fullerenes [40].) In the cases where the fullerene intercalated – such as with PC$_{61}$BM and PC$_{71}$BM – an excess of fullerene was required to make efficient devices. At a ratio of 1:1 PBTTT:fullerene, the fullerene completely intercalated between the side chains of the polymer; the absence of pure fullerene domains prevented the formation of a percolated net-work to transport electrons to the cathode. The efficiency of PBTTT:PC$_{71}$BM devices was optimized at a ratio of 1:4 [5,41,42]. That is, an excess of fullerene was necessary to form a percolated network of pure (or enriched) phases. While a large volume fraction of fullerene improved electronic performance, it also had a deleterious effect on the mechanical properties. Dauskardt, McGehee, and coworkers studied the effect of intercalation on the cohesion of poly(3,3‴-didodecyl quaterthiophene) (PQT-12) and PBTTT and found that high ratios of fullerenes (1:4) produced BHJ films with decreased cohesive energy compared to 1:1 blends [8]. A lower cohesive energy was also found in 1:1 blends with fullerene that did not intercalate (bis-PC$_{71}$BM) when compared to

blends with fullerene that did intercalate (PC$_{71}$BM) [8]. The lower cohesion was attributed to the weak van der Waals interactions in the fullerene-enriched phases; weakened intermolecular forces facilitated decohesion of the active layer [8].

3. Experimental design

3.1. Selection of materials

To isolate the effects of molecular mixing on the mechanical properties of polymer:fullerene blends from the effects of different mechanical properties inherent with different fullerenes, we used a single fullerene, PC$_{61}$BM, in our experiments. PC$_{61}$BM was selected because it is ubiquitous in literature and has previously been studied in blends with all of the polymers of this work [11,16,40,43]. We chose four different conjugated polymers for this work on the basis of the nature of the molecular mixing with fullerenes and the overall morphology of the bulk heterojunction. To summarize, P3HT and P3HpT are believed to form ternary blends comprising crystalline polymer phases, PC$_{61}$BM-enriched phases, and mixed phases. The principal difference in properties of the two polymer films is that the tensile modulus of P3HpT is about an order of magnitude lower than that of P3HT at ambient temperature [16]. PBTTT and PT2T have lower side chain densities than do the P3ATs, and thus permit intercalation of fullerenes. In the case of PBTTT, intercalation produces bimolecular crystallites [5,42]. In the case of PT2T, intercalation produces an amorphous, molecularly mixed blend [10,11].

3.2. Mechanical characterization

The tensile moduli of the neat polymer and 1:1 polymer: fullerene thin films were measured using the mechanical buckling technique originally described by Stafford et al. [44]. Under compressive strain on a relatively compliant substrate, a thin film forms a sinusoidal wrinkled or buckled pattern. The wavelength of the buckled pattern is then related to the tensile modulus. The distinct advantage of using the buckling technique is that it eliminates the difficulty of preparing and handling free-standing films ≤ 100 nm that would be required for conventional mechanical testing. The tensile modulus of the neat fullerene was difficult to measure by the buckling technique using a single layer of fullerene due to its brittleness. We instead determined the modulus using the bilayer buckling technique [45], which utilizes a second, more compliant layer with a modulus determined independently using the conventional single-layer buckling method (PEDOT:PSS), layered with the more brittle material of unknown modulus (in this case, PC$_{61}$BM).

The deviation from the rule of mixtures (or the volume fraction average) tensile modulus was calculated utilizing the simplex method first used by Kleiner to describe polymer composites [46]. This method allowed a qualitative description of the relative strength of interactions between the polymers and the PC$_{61}$BM.

3.3. UV–vis spectroscopy

To describe qualitatively the relative order within the thin films, we measured the absorption spectra of the polymers and polymer:fullerene blends, and compared the vibronic peaks associated with absorption of the aggregated (e.g., ordered) phases. We have previously applied the weakly interacting H-aggregate model to P3ATs and found that the aggregated phases of both P3HT and P3HpT have essentially identical degrees of extent and intra-aggregate order in neat polymer films [16]. Here, we did not use the H-aggregate model, but simply compared the differences in vibronic and maximum absorption peaks between thin films of neat polymer and polymer:fullerene blends before and after annealing.

3.4. Photovoltaic devices

We compared the photovoltaic properties of the polymers in 1:1 blends with PC$_{61}$BM as the electron acceptor. The ratio of 1:1 was selected to isolate the effects of molecular mixing and to limit the formation of pure fullerene phases. In the case of high molecular mixing, there is expected to be limited fullerene percolation pathways and a reduction in electron transport, as manifested in a low power conversion efficiency [40]. The transparent anode was spin-coated from a solution of PEDOT:PSS with 7% DMSO and 0.1% Zonyl fluorosurfactant (now called Capstone by Dupont) [47–49]. The top contact was a liquid metal cathode, eutectic gallium–indium (EGaIn), which was extruded from a syringe. We selected EGaIn because it has been shown to produce similar results as Al top contacts [50], allowed for rapid characterization of devices, and by nature of being a liquid metal, is stretchable [51].

4. Results and discussion

4.1. Mechanical properties of the neat polymers

The tensile moduli of the neat polymers were determined using the buckling method on thin films spin-coated from chloroform (Fig. 2). The tensile moduli of films of P3HT were found to be similar both as-cast (AC, 0.80 ± 0.12 GPa) and after annealing at 125 °C for 30 min (AN, 0.82 ± 0.05 GPa). P3HpT exhibited moduli that are about an order of magnitude lower than those of P3HT (0.082 ± 0.001 GPa as-cast and 0.130 ± 0.001 GPa after annealing at 100 °C for 30 min). We previously attributed the lower modulus of P3HpT to its side-chain length of seven carbon atoms to be the critical side-chain length for polythiophenes, that is, the critical side-chain length is the length at which T_g no longer drops monotonically with increasing side-chain length; $n=7$ is also the shortest side-chain length for which T_g is significantly below room temperature [16]. Because PT2T is very similar structurally to P3HT, it is not surprising that the two materials had nearly identical tensile moduli as-cast (1.07 ± 0.23 GPa) and after annealing at the same conditions (1.01 ± 0.27 GPa). The higher stiffness of PBTTT (2.90 ± 0.30 GPa) has been attributed to interdigitation of the side chains in the crystalline phase, and the fused
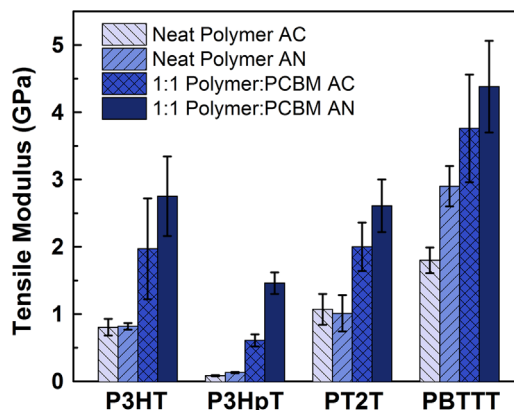

Fig. 2. Summary of the tensile moduli of both as-cast (AC) and annealed (AN) films. All were cast from CHCl$_3$. P3HpT was annealed at 100 °C, P3HT and PT2T were annealed at 125 °C, and PBTTT was annealed at 180 °C.

thienothiophene moieties between the separated bithiophene units along the backbone.

4.2. Mechanical properties of the polymer:fullerene blends

Organic photovoltaic devices (OPVs) are frequently fabricated with active layers comprising a conjugated polymer acting as an electron donor and a fullerene acting as the electron acceptor. Devices reported in literature often have polymer:fullerene blends with concentrations between 1:1 and 1:4. Because we were motivated to determine the effects of molecular mixing on

compliance, we decided to measure the tensile moduli of 1:1 polymer:fullerene blends (Fig. 2a). The ratio of 1:1 limits the formation of pure fullerene phases, which we were concerned would dominate the mechanical properties of the blend. P3HpT: $PC_{61}BM$ (0.61 ± 0.09 GPa AC, 1.46 ± 0.16 GPa AN) had the lowest moduli of all of the blends. The fullerene blends with P3HT (1.97 ± 0.75 GPa AC, 2.75 ± 0.59 GPa AN) and PT2T (2.00 ± 0.36 GPa AC, 2.61 ± 0.39 GPa AN) exhibited similar tensile moduli. This similarity is somewhat surprising considering the extent of molecular mixing is expected to be different for P3HT, which does not allow fullerene intercalation, and PT2T, which does allow
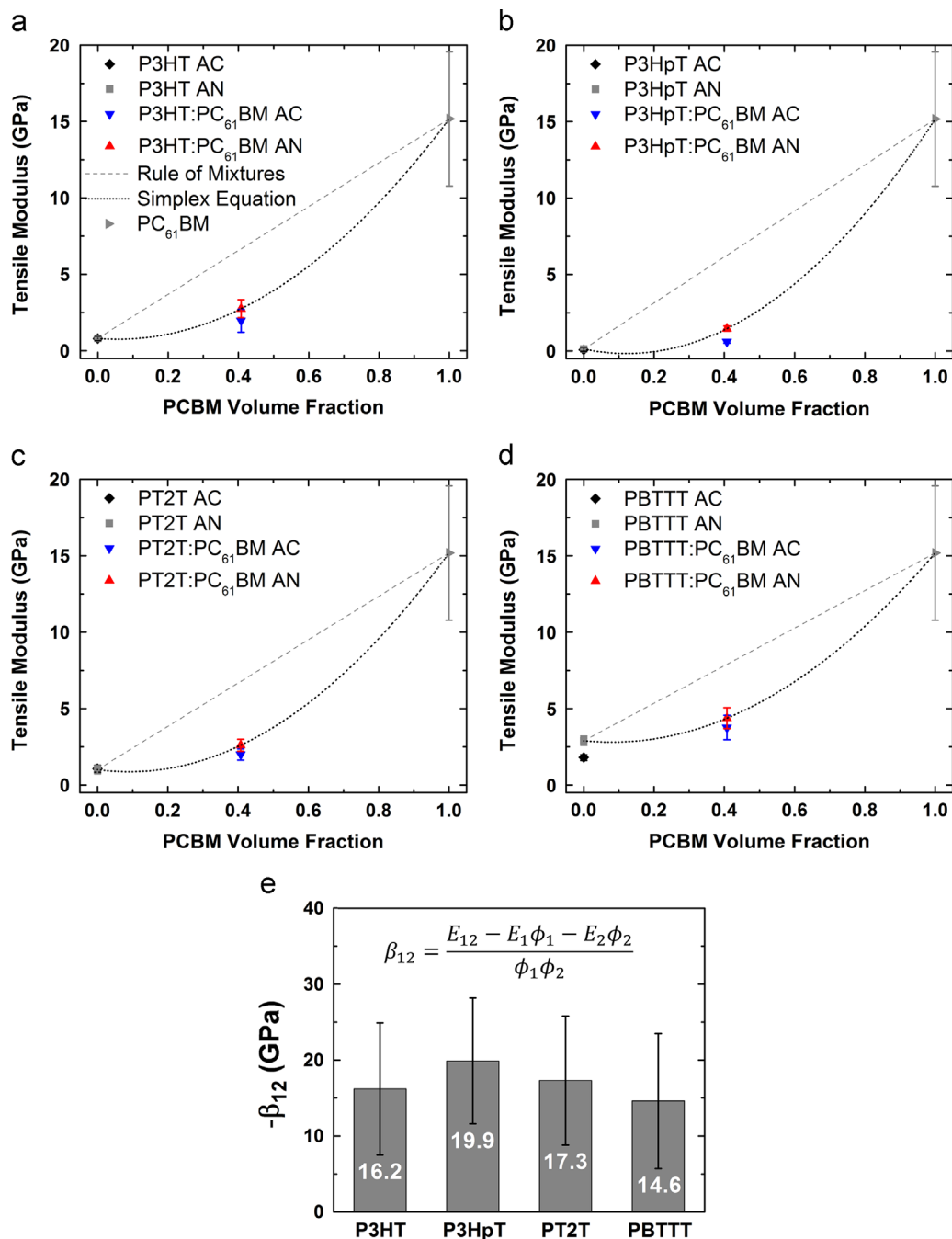

Fig. 3. The tensile moduli of the polymer:fullerene blends studied here deviate from the rule of mixtures. The volume fractions were calculated for the films and the interaction term, β_{12}, was determined from Eq. (1); the moduli for the neat polymer films as well as the fullerene blends are plotted here. Additionally, the rule of mixtures and the simplex equation moduli are plotted for all volume fractions of $PC_{61}BM$ for blends with (a) P3HT, (b) P3HpT, (c) PT2T, and (d) PBTTT. The negative of the calculated values of the interaction term, as well as the equation for calculating them, are shown in (e). The large error bars in (e) are a consequence of the error obtained when measuring the modulus of $PC_{61}BM$ by the bilayer bucking method; the uncertainty is in the absolute value, as opposed to in the qualitative ranking of the magnitude of the interaction term.

fullerene intercalation, and is in effect "all mixed". PBTTT, which also allows fullerene intercalation, was found to have the highest tensile modulus both as-cast (3.76 ± 0.80 GPa) and after annealing (4.38 ± 0.68 GPa). This stiffness can be attributed to the intercalation of the fullerenes and the subsequent reduction in free volume.

To compare how much stiffer films become upon addition of fullerene, we calculated the ratio of the tensile modulus of the polymer:fullerene blend to that of the neat polymer, E_{blend}/E_{poly} (Fig. 1). The factor by which the modulus of the P3HpT:PC$_{61}$BM blend was greater than that of the neat polymer was the highest of all four systems tested (7.44 ± 1.4 as-cast, 11.2 ± 1.5 after annealing). We attribute this high value to the anti-plasticizing effect of PC$_{61}$BM on the amorphous domains of P3HpT. Since P3HT (2.45 ± 1.0 as-cast, 3.37 ± 0.75 after annealing), PT2T (1.87 ± 0.52 as-cast, 2.58 ± 0.79 after annealing), and PBTTT (2.09 ± 0.50 as-cast, 1.51 ± 0.28 after annealing), are already in the glassy state at room temperature, the effect on the mechanical properties of the amorphous domains may have been masked.

Kleiner et al. showed that for a blend of two compatible glassy materials, the modulus can be described by a simplex equation in terms of the tensile moduli and volume fractions of the materials as well as an interaction energy between the materials [46]. The simplex equation describes the deviation of the blend modulus from the expected value based on the rule of mixtures, which is simply the average of the properties of the materials within the composite, weighted by volume fraction [9]. While P3HT, PT2T, and PBTTT are all glassy at room temperature, P3HpT is not [16]. However, it has been shown by others that the T_g of P3ATs increases with the addition of PCBM [16,19]. This increase in the T_g suggests that the simplex model is appropriate in describing the tensile modulus of P3HpT:PC$_{61}$BM blends.

Awartani et al. used the following simplex equation to describe the interaction energy between P3HT and PC$_{61}$BM [9]:

$$E_{12} = E_1\phi_1 + E_2\phi_2 + \beta_{12}\phi_1\phi_2 \qquad (1)$$

Here E_{12} is the modulus of the blend film, E_1 and E_2 are the moduli of the neat polymer and neat fullerene films, respectively, and ϕ_1 and ϕ_2 are the volume fractions of the polymer and fullerene. The volume fractions were calculated from reported densities of 1.1 g cm^{-3} for the thiophenes [52] and 1.6 g cm^{-3} for PC$_{61}$BM [52]. The interaction term, β_{12}, describes the deviation from the rule of mixtures. A positive interaction term may be attributed to an increase in crystallinity of the components when compared to the neat films, or a change in molecular packing resulting in a negative volume of mixing. A negative interaction term suggests opposite scenarios. The modulus of PC$_{61}$BM was 15.18 ± 4.39 GPa

as measured by the bilayer buckling method. This value is consistent with values of other small molecule semiconductors, such as pentacene, for which Tahk et al. obtained a modulus of 15 GPa by the buckling method [20]. We have also found that the moduli of PC$_{61}$BM is highly dependent on purity (i.e., the extent to which PC$_{71}$BM is removed from the mixture) [53]. While the uncertainty in the modulus of neat PC$_{61}$BM was high, it did not change our analysis because the sensitivity of the interaction term to the modulus of the PC$_{61}$BM is linear for all materials discussed here. This linear sensitivity means that even if we used the modulus of the fullerene measured by others (e.g., 3.06 GPa [9] or 6.2 GPa [34]), it would affect all of the interaction terms identically; that is, the values obtained for β_{12} would have the same qualitative ranking.

The tensile moduli of the polymers, fullerene, and polymer: fullerene blends, along with their moduli predicted on the basis of the rule of mixtures and the simplex equation are plotted in Fig. 3. After annealing, all of the polymer:fullerene blends had a negative interaction term. The lowest interaction term was observed in P3HpT (-19.9 ± 8.3 GPa). The interaction terms for P3HT (-16.2 ± 8.7 GPa) and PT2T (-17.3 ± 8.5 GPa) are relatively similar, while the interaction term for PBTTT is slightly higher (-14.6 ± 8.9 GPa). The higher interaction term of PBTTT is attributed to the negative volume of mixing due to intercalation.

4.3. Photovoltaic properties

The interaction term indicates a deviation from the rule of mixtures, but does not provide any insight as to the origin of the deviation. For example, blending could change the crystallization behavior of the pure phases. Bulk heterojunction OPVs need percolated networks of both donor and acceptor rich regions to separate charge and transport it to the electrodes. Intimate mixing of the polymer donor and fullerene acceptor can have deleterious effects on the creation of percolated networks for charge transport. To determine if these percolated networks were disrupted by extensive molecular mixing, photovoltaic devices were fabricated by mixing the polymers in a 1:1 ratio with PC$_{61}$BM (Fig. 4). Table 1 shows the figures of merit for the devices fabricated for this work. The power conversion efficiencies (PCE) of the devices comprising active layers of P3HT:PC$_{61}$BM and P3HpT:PC$_{61}$BM were $2.04 \pm 0.27\%$ and $2.16 \pm 0.17\%$, respectively, as previously reported [16]. The PCEs of PT2T:PC$_{61}$BM ($0.15 \pm 0.01\%$) and PBTTT:PC$_{61}$BM ($0.10 \pm 0.01\%$) devices were much lower. These low PCEs were attributed to a greater extent of molecular mixing than in P3HT and P3HpT; the high extent of molecular mixing prevents the formation of contiguous fullerene domains necessary for efficient charge transport to the cathode.
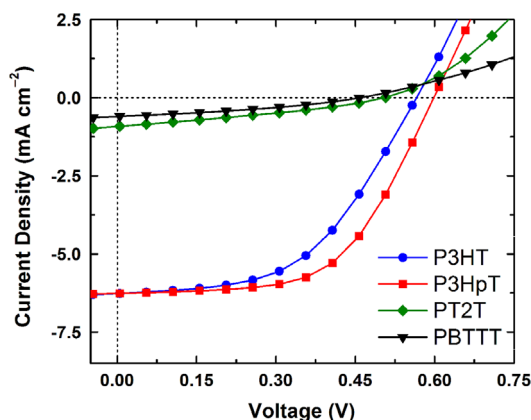

Fig. 4. *J–V* curves of the 1:1 polymer:fullerene blends spin-cast from ODCB. P3HpT: PC$_{61}$BM[a] devices were annealed at 100 °C for 30 min, P3HT:PC$_{61}$BM[a] and PT2T: PC$_{61}$BM devices were annealed at 125 °C for 30 min, and PBTTT:PC$_{61}$BM devices were annealed at 180 °C for 10 min. [a]Previously reported data from Ref. [16].

Table 1
Summary of the averaged figures of merit for the solar cells fabricated in this work ($N \geq 3$). The solar device architecture was PEDOT:PSS/polymer/PC$_{61}$BM/EGaIn. The active layer was spin-coated from a solution of 1:1 polymer:PC$_{61}$BM in ODCB. All devices were annealed at temperatures as described in the text in an inert atmosphere.

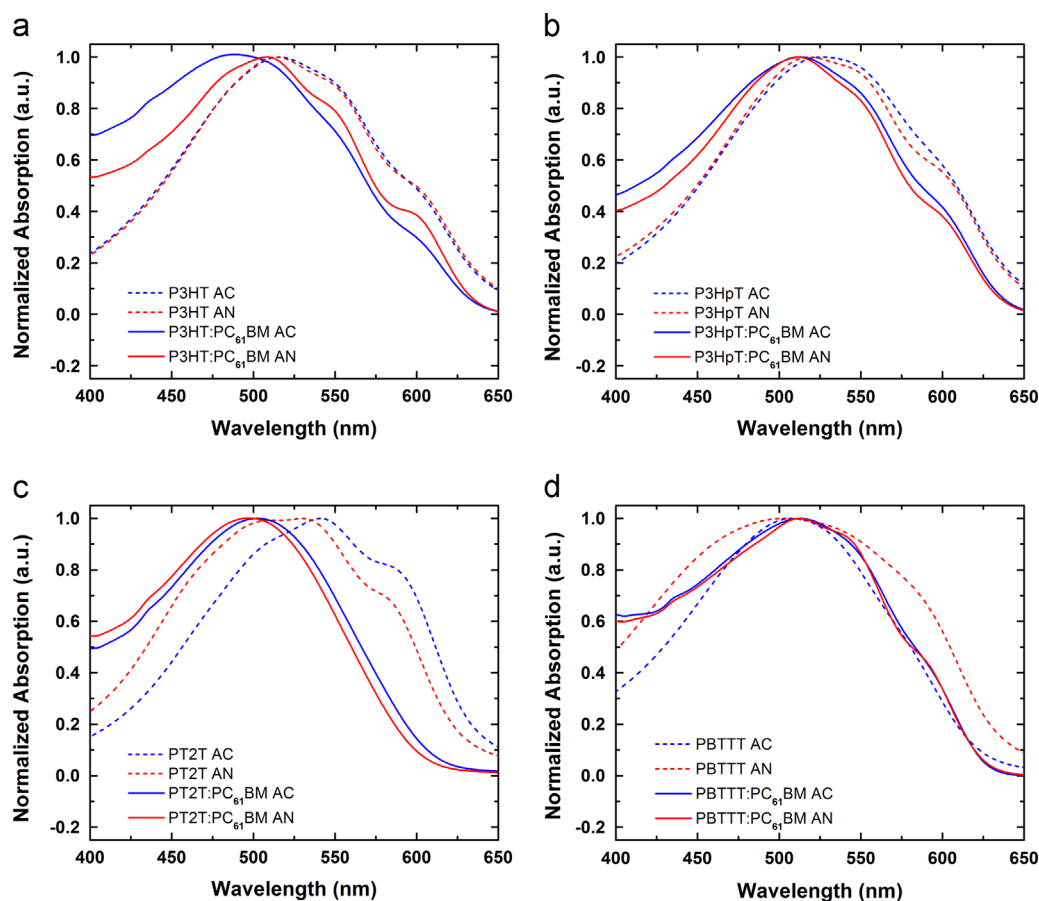| Materials	J_{sc} (mA cm^{-2})	V_{oc} (mV)	FF (%)	PCE (%)
P3HT[a]	6.95 ± 0.91	568 ± 9	51.7 ± 1.9	2.04 ± 0.27
P3HpT[a]	6.27 ± 0.48	598 ± 5	57.5 ± 1.8	2.16 ± 0.17
PT2T	0.92 ± 0.07	511 ± 28	31.7 ± 0.9	0.15 ± 0.01
PBTTT	0.60 ± 0.03	460 ± 20	35.1 ± 1.4	0.10 ± 0.01

[a] Previously reported data from Ref. [16].

Fig. 5. Absorption spectra of neat polymers and polymer:fullerene blends both as-cast (AC) and annealed (AN). (a) P3HT and 1:1 P3HT:PC$_{61}$BM; annealing was at 125 °C for 30 min. (b) P3HpT and 1:1 P3HpT:PC$_{61}$BM; annealing was at 100 °C for 30 min. (c) PT2T and 1:1 PT2T:PC$_{61}$BM; annealing was at 125 °C for 30 min. (d) PBTTT and 1:1 PBTTT:PC$_{61}$BM; annealing was at 180 °C for 10 min. All films were spin-coated from CHCl$_3$.

4.4. UV–vis absorption of the neat polymers and polymer:fullerene blends

The performance of OPV devices is heavily dependent on processing conditions [9]; therefore, OPV performance alone cannot describe the extent of molecular mixing in polymer:fullerene blends. To further examine the influence of the addition of PC$_{61}$BM on the order within the polymer phases, we measured the absorption spectra of thin films of the neat polymers and polymer:fullerene blends. Aggregated phases are evident (through vibronic transition peaks) in the absorption spectra of neat P3HT and P3HpT (Fig. 5a and b). When blended with the fullerene PC$_{61}$BM, these phases still exist, but the blue-shift in the maximum absorption peaks and the decrease in magnitude of the vibronic peaks at 550 and 605 nm for P3HT and P3HpT suggests that the conjugation length (which is a measure of quality within the aggregates) of the polymer decreases.

The absorption spectrum of neat PT2T (Fig. 5c), like P3HT, has observable vibronic transition peaks associated with the ordered phases. With the addition of PC$_{61}$BM, these vibronic peaks disappear and the absorption spectrum becomes broad and featureless, which is indicative of an amorphous polymer. The shift from ordered to amorphous polymer with the addition of PC$_{61}$BM is attributable to the fullerene intercalating between the side chains of PT2T and preventing crystalline lamellae from forming. Interestingly, PBTTT, which is another polymer that has been shown to allow fullerene intercalation, exhibits a qualitative change in order, but not a complete loss thereof (as determined by the absorption spectrum) with the addition of PC$_{61}$BM (Fig. 5d). We attribute the

difference in order between the two polymers that allow fullerene intercalation, PT2T and PBTTT, to the length of the side chains. The side chains of PT2T are six carbon atoms long, while those of PBTTT are 14 carbon atoms long. When the fullerene intercalates between the side chains of PT2T, the interactions between side chains are inhibited; the inhibition of side chain interactions disrupts the formation of stacks of lamellae, and thus crystallites, in PT2T. Conversely, the longer side chains in PBTTT reach past the intercalated fullerene and the van der Waals interactions between strands of PBTTT allow stacks of lamellae to form. This interpretation is consistent with the conclusions of McGehee and coworkers upon grazing-incidence X-ray diffraction studies of intercalated and non-intercalated blends [5,40,54].

4.5. Correlation between moduli of neat polymers and polymer:fullerene blends

Though the moduli of the polymer:fullerene blends deviates from the expected value based on the rule of mixtures, examination of Fig. 2 suggested that the moduli of the blends were correlated to the moduli of the neat polymers. Interestingly, the samples demonstrated a linear correlation ($R^2 = 0.97$ for as-cast, $R^2 = 0.95$ for annealed, Fig. 6). There is a decrease in slope of the linear fit from the as-cast films (Fig. 6a) to the annealed films (Fig. 6b). We attribute this observation – i.e., an apparent decreased dependence of the modulus of the blend on the modulus of the neat polymer upon thermal annealing – principally to two factors: (1) the large increase in modulus of P3HpT:PC$_{61}$BM compared to P3HpT upon thermal annealing (which reflects
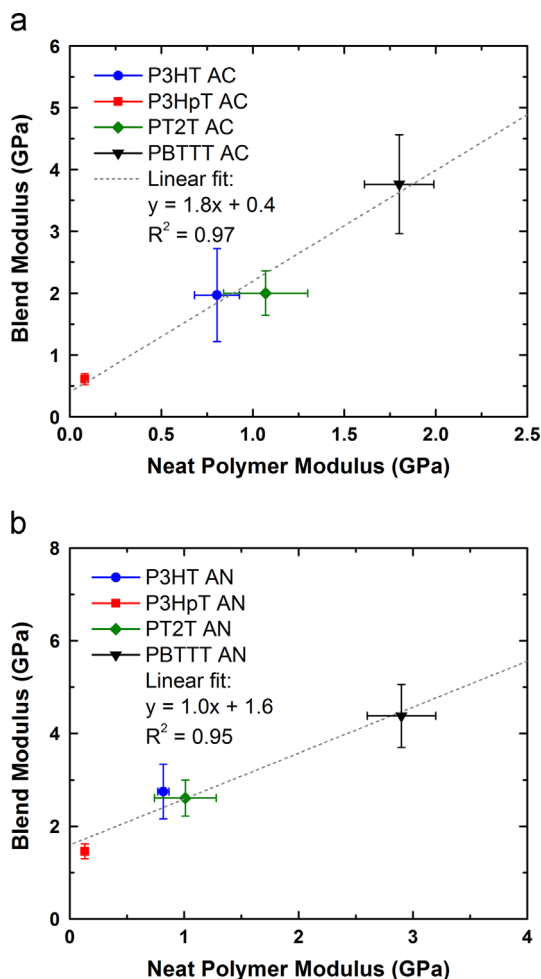
a

b

Fig. 6. Tensile moduli of the 1:1 polymer:fullerene blends versus moduli of the neat polymers for both (a) as-cast and (b) annealed films.

substantial enrichment of the fullerene phases and increased order in the polymer phases, possibly due to the increased fluidity of P3HpT chains compared to P3HT) and (2) the fact that PBTTT: PC$_{61}$BM films exhibit similar levels of order in both the as-cast and annealed films (as seen in Fig. 5d, which suggests a strong driving force for intercalation for these materials that is operative before thermal annealing). While it is possible that the linear correlation between the moduli of the polymer:fullerene blends and the moduli of the neat polymer of the materials studied here was coincidental, it at least warrants further investigation, and at most suggests a design rule for flexible OPV devices: the stiffness of the polymer substantially determines the stiffness of the blend. This conclusion seems intuitive, but perhaps not in light of the very different microstructures of the blended films.

5. Conclusion

This paper examined the effects of the extent of molecular mixing on the tensile modulus of polymer:fullerene blends. Unexpectedly, our analysis suggests that there is no direct correlation between the extent of molecular mixing and the tensile modulus or differential tensile modulus of polymer:fullerene blends. This observation is highlighted by the nearly identical tensile moduli of the structurally similar PT2T, which allows intercalation of PC$_{61}$BM, and P3HT, which prohibits intercalation. We also found a roughly linear correlation between the tensile

moduli of the polymer:fullerene blends to those of the neat polymers studied in this work. This correlation suggests that the molecular interactions that determine the tensile modulus of neat polymer films are dominant in determining the tensile modulus of polymer:fullerene blends.

Our findings suggest that for some polymers, the details of molecular mixing, while important to the electronic properties, apparently do not have an equally large effect on the stiffness of bulk heterojunction films. Although the extent of molecular mixing is evidently not a strong predictor for mechanical compliance for the materials tested in this work, the linear correlation between the tensile moduli of the neat polymer films and the polymer:fullerene blends suggests that flexibility and mechanical resilience can be tuned at the level of the polymer; while all polymer:fullerene blends reported so far have greater moduli than do the neat polymers, low-modulus polymers produce comparatively low-modulus blends. A greater understanding of the ways in which molecular mixing and phase separation dictate the mechanical properties of photoactive blends is of critical importance for the rational design of functional devices and for their stability in outdoor and portable environments.

6. Experimental

6.1. Materials

Poly(3-hexylthiophene) (P3HT, $M_w = 29,000$ g mol^{-1}, PDI=2.0) and [6,6]-phenyl C$_{61}$ butyric acid methyl ester (PC$_{61}$BM) were purchased from Sigma-Aldrich and used as received. Poly(3-heptylthiohene) (P3HpT, $M_w = 30,100$ g mol^{-1}, PDI=1.49) was purchased from Rieke Metals, Inc. Poly(2,5-bis(3-tetradecylthiophen-2-yl)thieno[3,2-b]thiophene) (PBTTT, $M_w = 23,000$ g mol^{-1}, PDI=1.9) was purchased from Solarmer Materials, Inc. and used as received. Poly-2,2′:5′,2″-(3,3″-dihexyl-terthiophene) (PT2T, $M_w = 19,400$ g mol^{-1}, PDI=1.31) was synthesized using previously established procedures [10,55]. Poly(dimethylsiloxane) (PDMS), Sylgard 184 (Dow Corning), was prepared according to the manufacturer's instructions at a ratio of 10:1 (base:crosslinker) and cured at room temperature for 36–48 h before it was used for mechanical testing. (Tridecafluoro-1,1,2,2-tetrahydrooctyl)-1-trichlorosilane (FOTS) was obtained from Gelest. Chloroform (CHCl$_3$), ortho-dichlorobenzene (ODCB), acetone, and isopropyl alcohol (IPA) were obtained from Sigma-Aldrich and used as received.

6.2. Preparation of substrates

Glass slides used as substrates for UV–vis spectrophotometry measurements were cut into 2.5 cm × 2.5 cm squares with a diamond-tipped scribe. They were then subsequently cleaned with Alconox solution (2 mg ml^{-1}), deionized water, acetone, and then isopropyl alcohol (IPA) in an ultrasonic bath for 10 min each and then rinsed and dried with compressed air. Next, the glass was plasma treated at $\sim$30 W for 3 min at a base pressure of 200 mTorr ambient air to remove residual organic material and activate the surface.

Glass slides used as substrates for thin films to be transferred to PDMS for buckle testing were prepared in the same manner as above, and then subsequently placed in a vacuum desiccator with a glass vial containing $\sim$100 μL of FOTS and put under house vacuum for a minimum of 3 h to passivate the surface.

6.3. Preparation of polymer solutions

Solutions of P3HT, P3HpT, PT2T, and PBTTT in CHCl$_3$ (7.5 mg ml^{-1}) and 1:1 polymer:PC$_{61}$BM (15.0 mg ml^{-1}) were prepared for the

buckling technique and UV–vis. Solutions of 1:1 P3HT:PC$_{61}$BM and P3HpT:PC$_{61}$BM (40 mg ml^{-1}), 1:1 PBTTT:PC$_{61}$BM (15 mg ml^{-1}), and 1:1 PT2T:PC$_{61}$BM (10 mg ml^{-1}) in ODCB were prepared for fabricating photovoltaic devices. All solutions were allowed to stir overnight (PBTTT and PBTTT:PC$_{61}$BM solutions were heated to 90 °C) and filtered with a 1-μm glass microfiber (GMF) syringe filter immediately before being spin-coated onto glass substrates.

6.4. Characterization of materials

The tensile moduli of the materials was measured with the buckling method as described elsewhere [21]. Briefly, the elastomer PDMS was chosen as the substrate for all tests. The PDMS was prepared as described above and then cut into rectangular strips ($l=8$ cm, $w=1$ cm, $h=0.3$ cm) before being stretched 4% using a computer-controlled linear actuator. While still under strain, FOTS treated glass slides (5 cm × 2.5 cm) were clipped onto the back of each strip using binder clips. To transfer the polymer or polymer: fullerene films to PDMS, the films were first spin-coated onto FOTS treated glass slides (2.5 cm × 2.5 cm) and then scored to facilitate transfer. The films were then placed against the PDMS, and after applying minimal pressure to achieve a conformal seal, the PDMS and glass slide with film were separated in one fast motion, leaving behind the film on the PDMS. After transfer, the PDMS substrates were relaxed; this action created a compressive strain that forced the conjugated polymer film to adopt sinusoidal buckles. The buckling wavelength, $\lambda_{\rm b}$, and the thickness of the film, $d_{\rm f}$, can be related to the tensile moduli of the film and the substrate, $E_{\rm f}$ and $E_{\rm s}$, and the Poisson ratios of the two materials, $\nu_{\rm f}$ and $\nu_{\rm s}$ by the following equation:

$$E_{\rm f} = 3E_{\rm s} \left(\frac{1-\nu_{\rm f}^2}{1-\nu_{\rm s}^2} \right) \left(\frac{\lambda_{\rm b}}{2\pi d_{\rm f}} \right)^3 \tag{2}$$

We measured the tensile modulus of the substrate, $E_{\rm s}$ (using a commercial pull tester), the buckling wavelength, $\lambda_{\rm b}$ (by optical microscopy), and the film thickness, $d_{\rm f}$ (by stylus profilometry). The slope of a plot of $\lambda_{\rm b}$ versus $d_{\rm f}$ for three different film thicknesses was inserted into Eq. (2). The Poisson's ratios were taken as 0.5 and 0.35 for PDMS and the conjugated polymers films, respectively. The experimental method is described in detail elsewhere.

Determination of the tensile modulus of PC$_{61}$BM was difficult using the method described above because of its propensity to crack upon transfer to the PDMS substrate. To measure this modulus, we instead used a bilayer buckling method. The bilayer buckling method entails measuring the tensile modulus of a bilayer film – one compliant layer with a known modulus layered with the more brittle material of unknown modulus. The effective modulus of the bilayer film is expressed with the following equation:

$$E_{\rm eff} = \frac{1+m^2n^4+2mn(2n^2+3n+2)}{(1+n)^3(1+mn)}E_1 \quad \text{where} \quad m=\frac{E_2}{E_1}, \quad n=\frac{h_2}{h_1} \tag{3}$$

where E_1 and E_2 are the moduli of the two films and h_1 and h_2 are the thicknesses of the two films. To calculate the modulus for PC$_{61}$BM, we mathematically solved the above equation using PEDOT:PSS as the layer with the known modulus.

6.5. Fabrication of solar cells

We deposited a layer of PEDOT:PSS from an aqueous solution containing 92.9 wt% Clevios PH 1000 (~0.9–1.2 wt% PEDOT:PSS), 7.0 wt% DMSO, and 0.1 wt% Zonyl fluorosurfactant as the transparent anode. The solution was filtered with a 1 μm glass microfiber syringe filter and then spin-coated at a speed of 500 rpm (250 rpm s^{-1} ramp) for 60 s, followed by 2000 rpm (750 rpm s^{-1} ramp) for 60 s. The samples were subsequently dried at 150 °C for 30 min. The photoactive layer was then spin-coated onto the electrode layer at a speed of 500 rpm (250 rpm s^{-1} ramp) for 240 s, followed by 2000 rpm (750 rpm s^{-1} ramp) for 60 s for the P3HT:PC$_{61}$BM and P3HpT:PC$_{61}$BM devices, and at a speed of 300 rpm (250 rpm s^{-1} ramp) for 240 s, followed by 2000 rpm (750 rpm s^{-1} ramp) for 60 s for all other devices. A thin strip of the PEDOT:PSS electrode was exposed by wiping away some of the photoactive layer with chloroform so that electrical contact could be made. The samples were then immediately placed in a nitrogen-filled glovebox. The P3HpT:PC$_{61}$BM samples were annealed at 100 °C for 30 min. The P3HT:PC$_{61}$BM and PT2T:PC$_{61}$BM samples were annealed at 125 °C for 30 min, while the PBTTT:PC$_{61}$BM samples were annealed at 180 °C for 10 min. All substrates were then allowed to cool slowly to room temperature. EGaIn (extruded by hand from a syringe) was used as the top contact. The photovoltaic properties were measured in a nitrogen-filled glovebox using a solar simulator with a 100 mW cm^{-2} flux that approximated the solar spectrum under AM 1.5G conditions (ABET Technologies 11,016-U up-facing unit calibrated with a reference cell with a KG5 filter). The current density versus voltage was measured for both dark and under illumination using a Keithley 2400 SourceMeter.

6.6. UV–vis spectroscopy

The absorbance of the materials was measured using a PerkinElmer Lambda 1050 UV–vis–NIR spectrophotometer. The wavelength range measured was 850–300 nm with a step size of 1 nm. The polymer solutions were spin-coated onto the glass slides at a spin speed of 500 rpm (250 rpm s^{-1} ramp) for 240 s followed by 2000 rpm (750 rpm s^{-1} ramp) for 60 s. For each solution, two films were prepared. The first film was left as-cast and the second film was heated at 100 °C for 30 min for P3HpT, 125 °C for 30 min for P3HT and PT2T, and 180 °C for 10 min for PBTTT. After heating, all samples were allowed to cool for at least 30 min under a Pyrex Petri dish covered in aluminum foil. All fullerene blends were prepared in the same manner as the neat polymer films.

References

[1] G. Yu, J. Gao, J.C. Hummelen, F. Wudl, A.J. Heeger, Polymer photovoltaic cells: enhanced efficiencies via a network of internal donor–acceptor heterojunctions, Science 270 (1995) 1789–1791.
[2] G. Dennler, M.C. Scharber, C.J. Brabec, Polymer–fullerene bulk-heterojunction solar cells, Adv. Mater. 21 (2009) 1323–1338.
[3] A.B. Tamayo, X.-D. Dang, B. Walker, J. Seo, T. Kent, T.-Q. Nguyen, A low band gap, solution processable oligothiophene with a dialkylated diketopyrrolopyrrole chromophore for use in bulk heterojunction solar cells, Appl. Phys. Lett. 94 (2009) 103301.
[4] P.M. Beaujuge, J.M.J. Fréchet, Molecular design and ordering effects in π-functional materials for transistor and solar cell applications, J. Am. Chem. Soc. 133 (2011) 20009–20029.
[5] A.C. Mayer, M.F. Toney, S.R. Scully, J. Rivnay, C.J. Brabec, M. Scharber, et al., Bimolecular crystals of fullerenes in conjugated polymers and the implications of molecular mixing for solar cells, Adv. Funct. Mater. 19 (2009) 1173–1179.

[6] M.T. Dang, L. Hirsch, G. Wantz, J.D. Wuest, Controlling the morphology and performance of bulk heterojunctions in solar cells. Lessons learned from the benchmark poly(3-hexylthiophene):[6,6]-phenyl-C61-butyric acid methyl ester system, Chem. Rev. 113 (2013) 3734–3765.

[7] D.J. Lipomi, Z. Bao, Stretchable, elastic materials and devices for solar energy conversion, Energy Environ. Sci. 4 (2011) 3314–3328.

[8] C. Bruner, N.C. Miller, M.D. McGehee, R.H. Dauskardt, Molecular intercalation and cohesion of organic bulk heterojunction photovoltaic devices, Adv. Funct. Mater. 23 (2013) 2863–2871.

[9] O. Awartani, B.I. Lemanski, H.W. Ro, L.J. Richter, D.M. DeLongchamp, B.T. O'Connor, Correlating stiffness, ductility, and morphology of polymer: fullerene films for solar cell applications, Adv. Energy Mater. 3 (2013) 399–406.

[10] M. Koppe, M. Scharber, C. Brabec, W. Duffy, M. Heeney, I. McCulloch, Poly-terthiophenes as donors for polymer solar cells, Adv. Funct. Mater. 17 (2007) 1371–1376.

[11] A.D. Printz, S. Savagatrup, D.J. Burke, T.N. Purdy, D.J. Lipomi, Increased elasticity of a low-bandgap conjugated copolymer by random segmentation for mechanically robust solar cells, RSC Adv. 4 (2014) 13635–13643.

[12] I. Mcculloch, M. Heeney, C. Bailey, K. Genevicius, I. Macdonald, M. Shkunov, et al., Liquid-crystalline semiconducting polymers with high charge-carrier mobility, Nat. Mater. 5 (2006) 328–333.

[13] N.C. Miller, E. Cho, R. Gysel, C. Risko, V. Coropceanu, C.E. Miller, et al., Factors governing intercalation of fullerenes and other small molecules between the side chains of semiconducting polymers used in solar cells, Adv. Energy Mater. 2 (2012) 1208–1217.

[14] R. Noriega, J. Rivnay, K. Vandewal, F.P.V. Koch, N. Stingelin, P. Smith, et al., A general relationship between disorder, aggregation and charge transport in conjugated polymers, Nat. Mater. 12 (2013) 1038–1044.

[15] M.A. Brady, G.M. Su, M.L. Chabinyc, Recent progress in the morphology of bulk heterojunction photovoltaics, Soft Matter 7 (2011) 11065–11077.

[16] S. Savagatrup, A.D. Printz, D. Rodriquez, D.J. Lipomi, Best of both worlds: conjugated polymers exhibiting good photovoltaic behavior and high tensile elasticity, Macromolecules 47 (2014) 1981–1992.

[17] S.T. Salammal, E. Mikayelyan, S. Grigorian, U. Pietsch, N. Koenen, U. Scherf, et al., Impact of thermal annealing on the semicrystalline nanomorphology of spin-coated thin films of regioregular poly(3-alkylthiophene)s as observed by high-resolution transmission electron microscopy and grazing incidence X-ray diffraction, Macromolecules 45 (2012) 5575–5585.

[18] J.Y. Kim, C.D. Frisbie, Correlation of phase behavior and charge transport in conjugated polymer/fullerene blends, J. Phys. Chem. C 112 (2008) 17726–17736.

[19] J. Zhao, A. Swinnen, G. Van Assche, J. Manca, D. Vanderzande, B. Van Mele, Phase diagram of P3HT/PCBM blends and its implication for the stability of morphology, J. Phys. Chem. B 113 (2009) 1587–1591.

[20] D. Tahk, H.H. Lee, D.-Y. Khang, Elastic moduli of organic electronic materials by the buckling method, Macromolecules 42 (2009) 7079–7083.

[21] S. Savagatrup, A.S. Makaram, D.J. Burke, D.J. Lipomi, Mechanical properties of conjugated polymers and polymer–fullerene composites as a function of molecular structure, Adv. Funct. Mater. 24 (2014) 1169–1181.

[22] S. Savagatrup, A.D. Printz, T.F. O'Connor, A.V. Zaretski, D.J. Lipomi, Molecularly stretchable electronics, Chem. Mater. 26 (2014) 3028–3041.

[23] C.W. Tang, Two-layer organic photovoltaic cell, Appl. Phys. Lett. 48 (1986) 183–185.

[24] N.S. Sariciftci, D. Braun, C. Zhang, V.I. Srdanov, A.J. Heeger, G. Stucky, et al., Semiconducting polymer–buckminster fullerene heterojunctions: diodes, photodiodes, and photovoltaic cells, Appl. Phys. Lett. 62 (1993) 585–587.

[25] S. Gu, H. Neugebauer, N.S. Sariciftci, S. Günes, Conjugated polymer-based organic solar cells, Chem. Rev. 107 (2007) 1324–1338.

[26] G. Zhao, Y. He, Y. Li, 6.5% Efficiency of polymer solar cells based on poly(3-hexylthiophene) and indene-C(60) bisadduct by device optimization, Adv. Mater. 22 (2010) 4355–4358.

[27] B. Walker, C. Kim, T.-Q. Nguyen, Small molecule solution-processed bulk heterojunction solar cells, Chem. Mater. 23 (2011) 470–482.

[28] N.D. Treat, M.L. Chabinyc, Phase separation in bulk heterojunctions of semiconducting polymers and fullerenes for photovoltaics, Annu. Rev. Phys. Chem. 65 (2014) 59–81.

[29] M. Hösel, R.R. Søndergaard, M. Jørgensen, F.C. Krebs, Failure modes and fast repair procedures in high voltage organic solar cell installations, Adv. Energy Mater. 4 (2014) 1301625.

[30] F.C. Krebs, T.D. Nielsen, J. Fyenbo, M. Wadstrøm, M.S. Pedersen, Manufacture, integration and demonstration of polymer solar cells in a lamp for the "Lighting Africa" initiative, Energy Environ. Sci. 3 (2010) 512–525.

[31] D. Chen, A. Nakahara, D. Wei, D. Nordlund, T.P. Russell, P3HT/PCBM bulk heterojunction organic photovoltaics: correlating efficiency and morphology, Nano Lett. 11 (2011) 561–567.

[32] S. van Bavel, E. Sourty, G. de With, K. Frolic, J. Loos, Relation between photoactive layer thickness, 3D morphology, and device performance in P3HT/PCBM bulk-heterojunction solar cells, Macromolecules 42 (2009) 7396–7403.

[33] N.D. Treat, M.A. Brady, G. Smith, M.F. Toney, E.J. Kramer, C.J. Hawker, et al., Interdiffusion of PCBM and P3HT reveals miscibility in a photovoltaically active blend, Adv. Energy Mater. 1 (2011) 82–89.

[34] D.-Y. Khang, J.A. Rogers, H.H. Lee, Mechanical buckling: mechanics, metrology, and stretchable electronics, Adv. Funct. Mater. 19 (2009) 1526–1536.

[35] B. O'Connor, E.P. Chan, C. Chan, B.R. Conrad, L.J. Richter, R.J. Kline, et al., Correlations between mechanical and electrical properties of polythiophenes, ACS Nano 4 (2010) 7538–7544.

[36] T.F. O'Connor, A.V. Zaretski, B.A. Shiravi, S. Savagatrup, A.D. Printz, M.I. Diaz, et al., Stretching and conformal bonding of organic solar cells to hemispherical surfaces, Energy Environ. Sci. 7 (2014) 370–378.

[37] D.J. Lipomi, H. Chong, M. Vosgueritchian, J. Mei, Z. Bao, Toward mechanically robust and intrinsically stretchable organic solar cells: evolution of photo-voltaic properties with tensile strain, Sol. Energy Mater. Sol. Cells 107 (2012) 355–365.

[38] J.D. Roehling, K.J. Batenburg, F.B. Swain, A.J. Moulé, I. Arslan, Three-dimensional concentration mapping of organic blends, Adv. Funct. Mater. 23 (2013) 2115–2122.

[39] N.D. Treat, A. Varotto, C.J. Takacs, N. Batara, M. Al-Hashimi, M.J. Heeney, et al., Polymer–fullerene miscibility: a metric for screening new materials for high-performance organic solar cells, J. Am. Chem. Soc. 134 (2012) 15869–15879.

[40] N.C. Miller, S. Sweetnam, E.T. Hoke, R. Gysel, C.E. Miller, J.A. Bartelt, et al., Molecular packing and solar cell performance in blends of polymers with a bisadduct fullerene, Nano Lett. 12 (2012) 1566–1570.

[41] N.C. Cates, R. Gysel, Z. Beiley, C.E. Miller, M.F. Toney, M. Heeney, et al., Tuning the properties of polymer bulk heterojunction solar cells by adjusting full-erene size to control intercalation, Nano Lett. 9 (2009) 4153–4157.

[42] N.C. Miller, R. Gysel, C.E. Miller, E. Verploegen, Z. Beiley, M. Heeney, et al., The phase behavior of a polymer–fullerene bulk heterojunction system that contains bimolecular crystals, J. Polym. Sci. Part B: Polym. Phys. 49 (2011) 499–503.

[43] P. Vanlaeke, A. Swinnen, I. Haeldermans, G. Vanhoyland, T. Aernouts, D. Cheyns, et al., P3HT/PCBM bulk heterojunction solar cells: relation between morphology and electro-optical characteristics, Sol. Energy Mater. Sol. Cells 90 (2006) 2150–2158.

[44] C.M. Stafford, C. Harrison, K.L. Beers, A. Karim, E.J. Amis, M.R. VanLandingham, et al., A buckling-based metrology for measuring the elastic moduli of polymeric thin films, Nat. Mater. 3 (2004) 545–550.

[45] C.M. Stafford, S. Guo, C. Harrison, M.Y.M. Chiang, Combinatorial and high-throughput measurements of the modulus of thin polymer films, Rev. Sci. Instrum. 76 (2005) 062207.

[46] L.W. Kleiner, F.E. Karasz, W.J. Macknight, Compatible glassy polyblends based upon poly(2,6-dimethyl-1,4-phenylene oxide): tensile modulus sudies, Polym. Eng. Sci. 19 (1979) 519–524.

[47] M. Vosgueritchian, D.J. Lipomi, Z. Bao, Highly conductive and transparent PEDOT:PSS films with a fluorosurfactant for stretchable and flexible transpar-ent electrodes, Adv. Funct. Mater. 22 (2012) 421–428.

[48] R.C. Chiechi, E.A. Weiss, M.D. Dickey, G.M. Whitesides, Eutectic gallium-indium (EGaIn): a moldable liquid metal for electrical characterization of self-assembled monolayers, Angew. Chem. Int. Ed. Engl. 47 (2008) 142–144.

[49] M.D. Dickey, R.C. Chiechi, R.J. Larsen, E.A. Weiss, D.A. Weitz, G.M. Whitesides, Eutectic gallium–indium (EGaIn): a liquid metal alloy for the formation of stable structures in microchannels at room temperature, Adv. Funct. Mater. 18 (2008) 1097–1104.

[50] A. Du Pasquier, S. Miller, M. Chhowalla, On the use of Ga–In eutectic and halogen light source for testing P3HT-PCBM organic solar cells, Sol. Energy Mater. Sol. Cells 90 (2006) 1828–1839.

[51] E. Palleau, S. Reece, S.C. Desai, M.E. Smith, M.D. Dickey, Self-healing stretchable wires for reconfigurable circuit wiring and 3D microfluidics, Adv. Mater. 25 (2013) 1589–1592.

[52] H.W. Ro, B. Akgun, B.T.O. Connor, M. Hammond, R.J. Kline, C.R. Snyder, et al., Poly(3-hexylthiophene) and [6,6]-phenyl-C61-butyric acid methyl ester mix-ing in organic solar cells, Macromolecules 45 (2012) 6587–6599.

[53] S. Savagatrup, D. Rodriquez, A.D. Printz, A.B. Sieval, J.C. Hummelen, D.J. Lipomi, Effect of fullerene size and mixed grades of [60]PCBM and [70]PCBM on the mechanical properties of bulk heterojunction films (2014) (submitted for publication).

[54] N.C. Miller, E. Cho, M.J.N. Junk, R. Gysel, C. Risko, D. Kim, et al., Use of X-ray diffraction, molecular simulations, and spectroscopy to determine the mole-cular packing in a polymer–fullerene bimolecular crystal, Adv. Mater. 24 (2012) 6071–6079.

[55] S. Tierney, M. Heeney, I. McCulloch, Microwave-assisted synthesis of poly-thiophenes via the Stille coupling, Synth. Met. 148 (2005) 195–198.